Journal of Physics: Condensed Matter

PAPER

# Infrared lattice dynamics in negative thermal expansion material in single-crystal $ScF_3$

To cite this article: Sahan U Handunkanda *et al* 2020 *J. Phys.: Condens. Matter* **32** 035403



IOP Publishing Journal of Physics: Condensed Matter
J. Phys.: Condens. Matter **32** (2020) 035403 (6pp) https://doi.org/10.1088/1361-648X/ab4955

# Infrared lattice dynamics in negative thermal expansion material in single-crystal $ScF_3$

**Sahan U Handunkanda[1,2], Erin B Curry[1], Vladimir Voronov[3] and Jason N Hancock[1,2]**

[1] Department of Physics, University of Connecticut, Storrs, CT 06269, United States of America
[2] Institute for Materials Science, University of Connecticut, Storrs, CT 06269, United States of America
[3] Laboratory of Crystal Physics, Kirensky Institute of Physics, Federal Research Center KSC SB RAS, Krasnoyarsk 660036, Russia

E-mail: jason.hancock@uconn.edu

Received 1 August 2019, revised 20 September 2019
Accepted for publication 30 September 2019
Published 23 October 2019

**Abstract**

Simple cubic 'open' perovskite $ScF_3$ stands out among trifluoride materials in its large, isotropic negative thermal expansion (NTE), but also its proximity of its zero-temperature state to a structural phase transition. Here we report a temperature- and frequency-dependent lattice dynamical study of Brillouin zone center lattice excitations of single crystals of $ScF_3$ using infrared reflectivity measurements. In addition to quantifying the mode strengths and energies in single crystals of this interesting material, we also find strong evidence for multiphonon absorption processes which excite the zone-edge incipient soft modes associated with NTE and the structural quantum phase transition. In this way, we identify an optically-allowed pathway to excite soft modes provides a means to athermally populate modes associated with NTE in $ScF_3$.

Keywords: phonons, infrared reflectivity, negative thermal expansion, optical properties

(Some figures may appear in colour only in the online journal)

## 1. Introduction

Since the discovery of strong, thermally persistent, isotropic negative thermal expansion (NTE) in $ZrW_2O_8$ in the 1990s, several new materials have shown similarly astonishing effects manifest in much simpler structures [1–6]. In all of these systems, low levels of hydrostatic pressure can induce a structural transformation, either through symmetry breaking or amorphization [7–13], suggestive that competing instabilities may be important to the robust NTE effect in these systems. Perhaps the structurally simplest member of this family is $ScF_3$, which may be classified as an ionic insulator, free of magnetism and mobile carriers [14], so falls into the class of structural negative thermal expansion (SNTE) materials [3, 15, 16] where purely lattice degrees of freedom are responsible for the anomalous mechanical behavior. $ScF_3$ is a perovskite, a structural class whose instabilities have been carefully studied in the ferroelectric community and categorized according to octahedral tilting schemes and the associated modes are natural candidates for driving SNTE.

Recently, signatures of an approach to an incipient lower-symmetry structural phase were detected using inelastic x-ray scattering (IXS) [3]. Specifically, incipient soft modes circumscribing the edges of the simple-cubic Brillouin zone (BZ) were observed to soften toward zero frequency at an extrapolated temperature $T = -39$ K. These observations constitute the most direct evidence that SNTE in this system emerges from a structural quantum phase transition. In this work, we extend these studies using high-resolution table-top infrared (IR) spectroscopy.

 

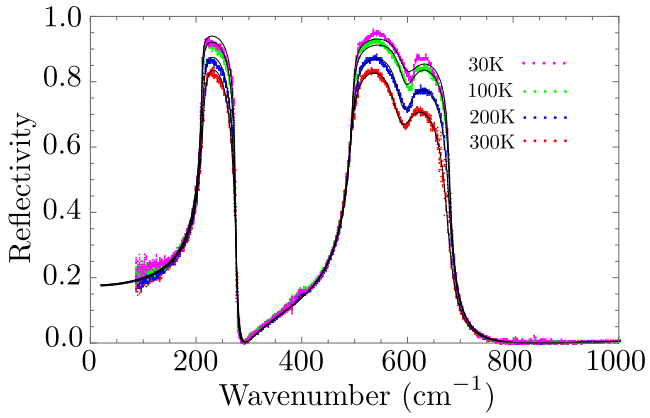


**Figure 1.** Temperature-dependent IR reflectivity data from single crystal $ScF_3$ and corresponding fits (black solid lines) using equation (1).

## 2. Experimental details

IR measurements were carried out using single crystalline $ScF_3$ grown using the flux technique as described previously [17, 18] and a 3 mm × 1.5 mm × 1 mm single crystal sample was carefully polished to a mirror-like surface. The polished surface was half-coated with gold using thermal evaporation. At each temperature, high resolution 0.5 cm$^{-1}$ far-IR spectra were collected through a 1.3 mm aperture from both the sample and gold reference surface using a Bruker 66v Fourier transform infrared spectrometer (FTIR). Reflectivity was calculated by dividing the spectra collected from the sample and gold reference. The sample was kept under vacuum in an optical continuous flow cryostat cooled using liquid helium while the sample temperature was measured using a Cernox sensor mounted near the sample. The spectra were collected using bolometeric detection covering the range of frequencies 100–1000 cm$^{-1}$ using a multilayer beam splitter and a glow-bar as radiation source.

## 3. Infrared reflectivity

Reflectivity data shown in figure 1 shows two strong rest-strahlen bands, which are clear signatures of dipole-active phonon modes at the simple cubic BZ center. The cubic structure of perovskite $ScF_3$ has the symmetry of the $Pm\bar{3}m$ space group. Considering the Sc and F atoms occupy the Wyckoff positions 1a (0,0,0) and 3d (1/2,0,0) in a four-atom unit cell, we anticipate 12 phonon branches. The irreducible representations at the BZ center factorize as $T_{2u} + 3T_{1u}$ [17] where a $T_{1u}$ representation corresponds to three acoustic modes and the remaining $T_{2u} + 2T_{1u}$ are optical modes. Among these, two $T_{1u}$ modes are infrared active, none are Raman active, and the $T_{2u}$ mode is silent.

We have used Kramers–Kronig-consistent analysis [19] to analyze the fundamental response functions $\epsilon(\omega)$ at each temperature from our frequency-dependent reflectivity data. Figure 2 shows the temperature evolution of the imaginary part of the dielectric function, Im($\epsilon(\omega)$) and the imaginary part of the loss function, Im($-1/\epsilon(\omega)$). In general, the poles

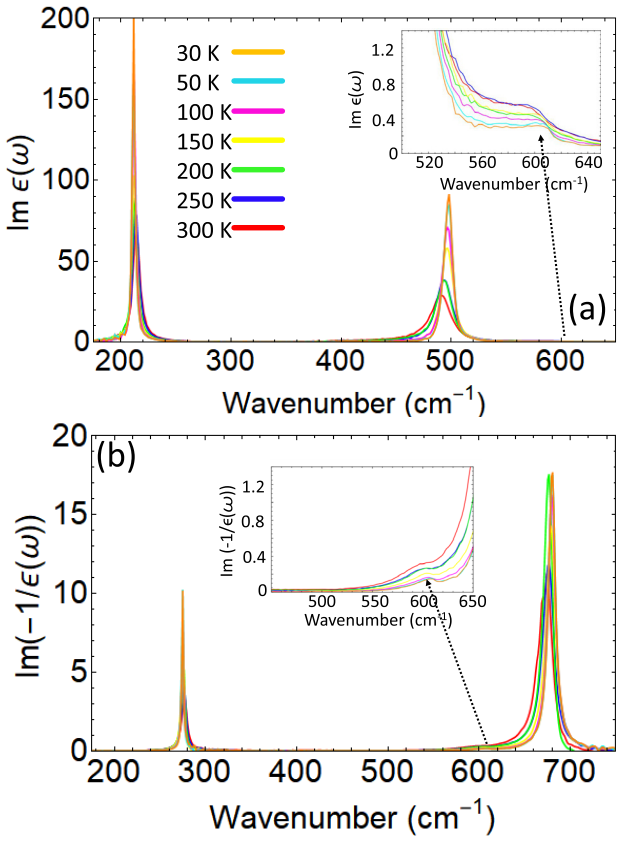


**Figure 2.** (a) Peaks in the temperature dependent Im $\epsilon(\omega)$ correspond to TO phonon peaks. (b) Peak in the temperature-dependent loss function, − 1/Im $\epsilon(\omega)$ correspond to LO phonon peaks. The insets of (a) and (b) detail the multiphonon absorption features.

of $\epsilon(\omega)$ are identified as transverse optical (TO) phonon frequencies and the poles of Im($-1/\epsilon(\omega)$) represent longitudinal optical (LO) phonons. Clear signatures of a third pole, or weak set of poles in $\epsilon(\omega)$ around 600 cm$^{-1}$ in figure 2 is not expected from the group theoretical treatment of zone-center (ZC) single phonon absorption and we assign this to multiphonon absorption, discussed further below.

For non-polar crystals, IR active modes are triply degenerate with two TO and one LO mode in each branch. For polar crystals, as expected for $ScF_3$, the TO and LO modes can be split significantly at ZC due to the long-range nature of the unscreened Coulomb interaction. When this LO-TO splitting is large, different decay channels could be expected for LO and TO modes. In order to account for this difference, we consider the factorized form of the dielectric function which allows different dissipation for LO and TO modes, as is shown in previous studies [20–24] of polar crystals. The temperature-dependent IR reflectivity data was therefore fit using a model dielectric function of the form

$$\epsilon(\omega) = \epsilon_\infty \prod_n \frac{\omega_{\mathrm{LO}n}^2 - \omega^2 - \mathrm{i}\omega\gamma_{\mathrm{LO}n}}{\omega_{\mathrm{TO}n}^2 - \omega^2 - \mathrm{i}\omega\gamma_{\mathrm{TO}n}} \qquad (1)$$

where $\omega_{\mathrm{TO}n}$ is the $n$th transverse vibrational mode frequency and $\omega_{\mathrm{LO}n}$ is $n$th longitudinal vibrational mode frequency, $\gamma_{\mathrm{LO}n}$ and $\gamma_{\mathrm{TO}n}$ are the corresponding damping parameters, and $\epsilon_\infty$

**Table 1.** Comparison of our experimental results for single crystal $ScF_3$ with previous calculations and experiments at 300 K. Mode frequencies are expressed in $cm^{-1}$. The experiments of [4] cite the peaks of absorption, which are between the TO and LO mode frequencies.

| Source | $\omega_{TO1}$ | $\omega_{LO1}$ | $\omega_{TO2}$ | $\omega_{LO2}$ |
|---|---|---|---|---|
| Expt.[Ours] | 214.0 | 276.9 | 493.4 | 675.3 |
| Calc. [4] | 217.5 | ∼275 | 486.8 | ∼695 |
| Expt. [4] | 220 | | 520 | |
| Calc. [2] | ∼190 | ∼359 | ∼496 | ∼665 |
| Calc. [32] | ∼200 | — | ∼450 | — |
| Calc. [18] | 211 | 154 | 477 | 590 |
| Calc. [33] | ∼200 | ∼260 | ∼467 | ∼673 |

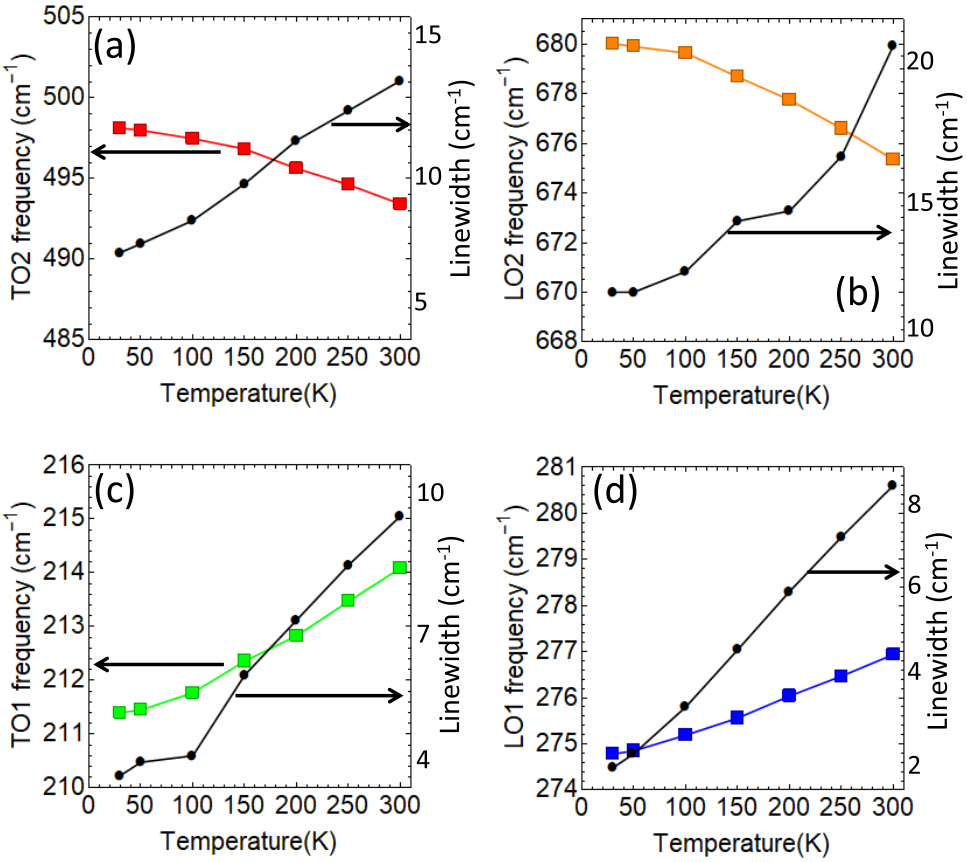


**Figure 3.** Temperature-dependent phonon frequencies and linewidths for the salient modes: (a) TO2, (b) LO2, (c) TO1, and (d) LO1 phonons obtained by fitting the raw reflectivity data at different temperatures.

is the high-frequency dielectric constant. The resultant fits are plotted along with the experimental data in figure 1.

The value $\epsilon_\infty = 1.92$ obtained from fitting is between a previously-reported theoretical value of 1.84 [4] and a value determined using spectral ellipsometry on thin polycrystalline films in the near infrared [25]. In this experimental work, the longest 700 nm wavelength result is $\epsilon = 2.11$, and the Sellmeier-extrapolated value at 1000 $cm^{-1}$ is $\epsilon_\infty = 2.09$. These low values are expected as a consequence of the large band gap (>9 eV) [26] and the Lyddane–Sachs–Teller relation [27]. In addition to the salient $T_{1u}$ modes (TO1 at 214 $cm^{-1}$ and TO2 mode at 495 $cm^{-1}$), we address the strong multiphonon absorption feature within the broad reststrahlen band near 600 $cm^{-1}$ by including a single additional oscillator ($n = 3$).

Although no IR reflectivity study of single crystalline transition metal trifluorides exists in the literature to our knowledge, the phonon frequencies at ZC have been calculated [28] for trifluorides $InF_3$, $GaF_3$ and $AlF_3$ in the cubic $Pm\bar{3}m$ phase and the reported LO-TO splittings are much smaller than the values obtained for $ScF_3$. Following Zhong *et al* [29], large LO-TO splitting can be attributed to large Born effective charges in $ScF_3$ [30] ($Z^*$(Sc) =3.99 and $\langle Z^*(F)\rangle = -1.33$) compared with other trifluorides [28][4]. We note that $ScF_3$ has no free electronic carriers, which would tend to screen the LO-TO splitting if present [31].

[4] For $AlF_3$, $Z^*(Al) = 3.08$ and $\langle Z^*(F)\rangle = -1.21$, for $GaF_3$, $Z^*(Ga) = 2.87$, $\langle Z^*(F)\rangle = -1.05$ and for $InF_3$, $Z^*(In) = 2.99$, $\langle Z^*(F)\rangle = -1.1$.

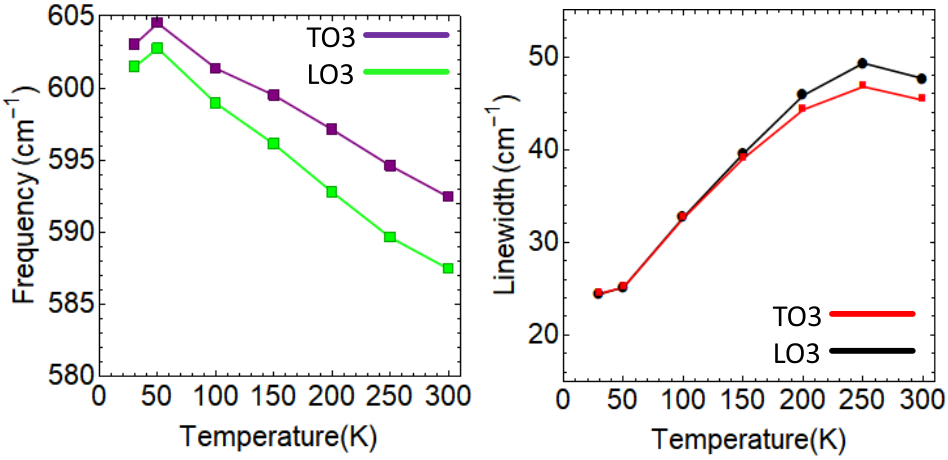


**Figure 4.** Temperature-dependent fit parameters quantifying the observed multiphonon absorption: (a) multiphonon frequencies and (b) multiphonon linewidths.

Table 1 compares the results for the mode energies at ambient temperature along with prior published calculations [2, 4, 18, 32, 33] and measurements [4]. The absorbance calculated from our Kramers–Kronig consistent analysis of $\epsilon(\omega)$ [19] appears in accord with Piskunov *et al* [4], who reports absorption peaks through a commercial polycrystalline $ScF_3$ powder sample but do not experimentally resolve the LO-TO splitting. Figure 3 plots the temperature-dependent fit parameters for the salient modes and shows that upon cooling, the low frequency Sc–F–Sc bond bending TO1 (LO1) mode softens about 3 cm$^{-1}$ (2 cm$^{-1}$), while the TO2 and LO2 bond stretch mode conversely stiffens by about 5 cm$^{-1}$, in rough agreement with [4]. A sharp and well-isolated peak in a neutron time-of-flight density of states (DOS) measurement is in strong accord with our TO2 mode in both frequency and temperature dependence between 300 K and base temperature [2]. Overall, the linewidths obtained for TO2/LO2 modes are greater than the TO1/LO1 modes suggesting the $n = 2$ phonons are more strongly coupled to other modes than the $n = 1$ phonons, a point discussed in more detail below.

The fitting parameters corresponding to the $n = 3$ modes are shown in figure 4. The large line widths and strongly temperature-dependent width and position compared to the salient modes supports the $n = 3$ absorption as arising from a set of kinematically-constrained multiphonon processes. The best-studied multiphonon processes known in the context of polar compounds are often discussed as arising from lattice anharmonicity or high-order dipole moment [24, 34–36]. The extreme anharmonicity present in $ScF_3$ and related materials [2], particularly for modes at BZ edge, suggests an intriguing possibility for the ZC absorption we have uncovered here.

Multiphonon absorption features are commonly observed in the infrared response of oxide and fluoride materials [23, 24, 37–41]. Only in select cases have a full-scale calculation including phonon scattering matrix elements and their coupling to radiation have been attempted [42, 43]. In the case of cubic insulating LiF [42] and other cubic halides [43], where these effects have been exhaustively explored in quantitative detail using the deformation dipole approach, weak sidebands appear to be well-described by two-phonon absorption. Here, an incoming photon with frequency $\omega_\gamma$ and negligible momentum $\mathbf{q}_\gamma \sim 0$ produces two phonons with opposite momenta, $\mathbf{q}$ and $-\mathbf{q}$. The energy is similarly conserved, up to interaction self energy of the two phonons produced.

The multiphonon absorption feature in $ScF_3$ near 600 cm$^{-1}$ appears as a sideband of the $n = 2$ modes and we consider both difference and sum frequency satellites respectively of the LO2 and TO2 modes. Because the multiphonon feature persists to low temperature, a difference frequency satellite of the LO2 modes seems untenable. Rather, following others [24], we suggest that the multiphonon feature in $ScF_3$ is in fact a sum frequency sideband of the TO2 mode and consider which modes are most likely coupled.

The main multiphonon feature peaks at about 100 cm$^{-1}$ above the TO2 mode, with significant absorption persisting down to the TO2 mode frequency. This frequency difference corresponds well with the lowest peak in the measured phonon DOS [2] near 105 cm$^{-1}$, which is also observed to slightly stiffen, about 3% upon cooling from 750 K to 7 K. According to lattice dynamical calculations, this peak is a van Hove singularity comprised of mainly acoustic modes [2, 4, 18, 33]. While these data display a smooth tail below 80 cm$^{-1}$ peak consistent with purely Debye contributions, momentum-resolved IXS work [3] clearly reveals the detailed phonon dispersion in $ScF_3$ is far richer, with low-frequency optical modes as low as 8 cm$^{-1}$, as indicated via many computational efforts [2, 4, 18, 33]. The IXS data show incipient soft optical modes well below 80 cm$^{-1}$ and along a set of momenta within a 1D manifold that circumscribes the entire cubic BZ boundary. At room temperature, this manifold of modes along the $M - R$ cut of the simple cubic BZ have frequency $\omega \sim 28$ cm$^{-1}$, softening nearly uniformly to less than 8 cm$^{-1}$ at cryogenic temperatures. Modes along this high-symmetry cut are often described as octahedral tilts, and when they soften, are responsible for the wide variation in low-symmetry structures condensing from higher temperature $Pm\bar{3}m$ cubic perovskites. Unusually, $ScF_3$ has no such symmetry-lowering transition, a fact that we have discussed as central to the physics of materials in this class, underpinning the strong, isotropic, and thermally-persistent SNTE in this system [3]. The apparent

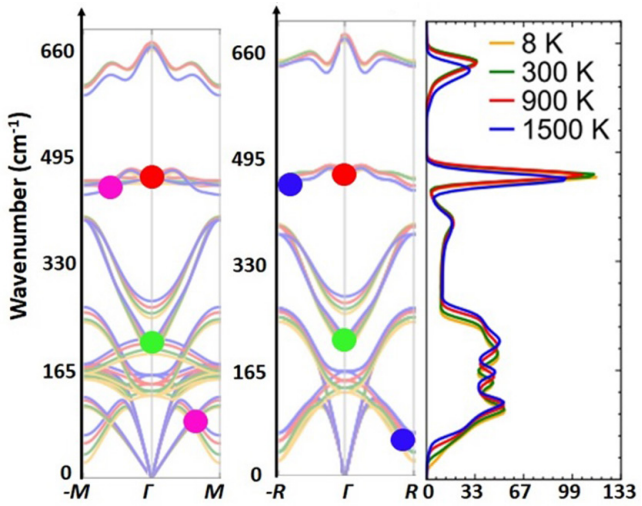


**Figure 5.** Schematic of the phonon band structure of $ScF_3$ following [33]. Green and red circles respectively indicate the TO1 and TO2 ZC phonon modes. Purple (blue) circles show representative $\mathbf{q}/-\mathbf{q}$ phonon pairs which contribute to two-phonon absorption near 600 $cm^{-1}$. Here, one phonon lies in the flat TO2 branch and the other lies near the incipient soft modes at the $M$ ($R$) point. The right panel shows the DOS calculated from the dispersion and the van Hove singularity near 500 $cm^{-1}$.

photon-induced creation of optical phonons at low energy, illustrated schematically in figure 5, raises an intriguing possibility that one may identify an inroad to optically excite the softest modes in the system near the zone boundary.

Radiative coupling to zone-edge modes through optical means opens an interesting possibility of producing athermal population of the incipient soft modes responsible for SNTE. With ultrashort pulses produced by x-ray free electron lasers [44, 45], experiments aimed to study dynamical processes in real time can be realized. One may expect unusual strain states to be produced by local optical pumping, and genesis of strain waves as a relaxation process. Furthermore, the detailed lattice dynamics and interesting phenomena such as the central peak can be examined in real time.

Deliberate laser-based athermal population of incipient modes near the $M-R$ manifold could also produce local shrinking of the crystal and a nonuniform strain state within and around the illuminated region. Because the system is at the precipice of a structural instability, one may observe domain writing into the lower-symmetry rhombohedral phase if a suitable laser source can be identified. Domain control at the nanoscale has been realized using different microscopic techniques [46–49] in ferroelectric, ferroelastic and ferromagnetic materials with a macroscopic electric or magnetic dipole moment. If realized, direct domain writing using mutliphonon absorption near an antiferrodistortive transition may bring distinct advantages particularly in the area of mechanical metamaterials. The contrast between equilibrium volume and elastic stiffness on crossing the cubic-to-rhombohedral structural phase boundary could be used to form microscopic elastic textures enabling bulk metamechanical responses not currently available from either constituent phase.

We have carried out IR reflection spectroscopy measurement in single crystal $ScF_3$. Temperature dependence of transverse and longitudinal optics modes are obtained and results very well agree with previous calculations. Multiphonon absorption in ionic halide systems are common and we have observed evidence of a two-phonon absorption for the first time in $ScF_3$. We propose this two-phonon absorption feature directly produces incipient soft modes residing at the BZ edge and propose an experiment for further investigation.

## Acknowledgments

Work at the University of Connecticut is supported by National Science Foundation Award No. DMR-1506825.

## ORCID iDs

Jason N Hancock https://orcid.org/0000-0003-1101-8962

## References

[1] Greve B K, Martin K L, Lee P L, Chupas P J, Chapman K W and Wilkinson A P 2010 *J. Am. Chem. Soc.* **132** 15496
[2] Li C W, Tang X, Munoz J A, Keith J B, Tracy S J, Abernathy D L and Fultz B 2011 *Phys. Rev. Lett.* **107** 195504
[3] Handunkanda S U, Curry E B, Voronov V, Said A H, Guzmán-Verri G G, Brierley R T, Littlewood P B and Hancock J N 2015 *Phys. Rev.* B **92** 134101
[4] Piskunov S, Žguns P A, Bocharov D, Kuzmin A, Purans J, Kalinko A, Evarestov R A, Ali S E and Rocca F 2016 *Phys. Rev.* B **93** 214101
[5] Hu L, Chen J, Sanson A, Wu H, Guglieri Rodriguez C, Olivi L, Ren Y, Fan L, Deng J and Xing X 2016 *J. Am. Chem. Soc.* **138** 8320
[6] Lazar P, Bučko T and Hafner J 2015 *Phys. Rev.* B **92** 224302
[7] Keen D A, Goodwin A L, Tucker M G, Dove M T, Evans J S, Crichton W A and Brunelli M 2007 *Phys. Rev. Lett.* **98** 225501
[8] Pantea C, Migliori A, Littlewood P, Zhao Y, Ledbetter H, Lashley J, Kimura T, Van Duijn J and Kowach G 2006 *Phys. Rev.* B **73** 214118
[9] Jørgensen J E, Staun Olsen J and Gerward L 2000 *J. Appl. Crystallogr.* **33** 279
[10] Chatterji T, Freeman P, Jimenez-Ruiz M, Mittal R and Chaplot S 2009 *Phys. Rev.* B **79** 184302
[11] Božin E, Chatterji T and Billinge S J 2012 *Phys. Rev.* B **86** 094110
[12] Zhou W, Wu H, Yildirim T, Simpson J R and Walker A H 2008 *Phys. Rev.* B **78** 054114
[13] Han S S and Goddard W A 2007 *J. Phys. Chem.* C **111** 15185
[14] Hu L *et al* 2015 *Adv. Mater.* **27** 4592
[15] Handunkanda S U, Occhialini C A, Said A H and Hancock J N 2016 *Phys. Rev.* B **94** 214102
[16] Occhialini C A, Handunkanda S U, Said A, Trivedi S, Guzman-Verri G G and Hancock J N 2017 *Phys. Rev. Mater.* **1** 070603
[17] Aleksandrov K, Voronov V, Vtyurin A, Krylov A, Molokeev M, Pavlovski M, Goryanov S, Likhacheva A Y and Ancharov A 2009 *Phys. Solid State* **51** 810
[18] Aleksandrov K, Voronov V, Vtyurin A, Goryainov S, Zamkova N, Zinenko V and Krylov A 2002 *J. Exp. Theor. Phys.* **94** 977

[19] Kuzmenko A 2005 *Rev. Sci. Instrum.* **76** 083108
[20] Berreman D W and Unterwald F 1968 *Phys. Rev.* **174** 791
[21] Lowndes R 1970 *Phys. Rev.* B **1** 2754
[22] Kurosawa T 1961 *J. Phys. Soc. Japan* **16** 1298
[23] Gervais F and Piriou B 1974 *Phys. Rev.* B **10** 1642
[24] Willett-Gies T I, Nelson C M, Abdallah L S and Zollner S 2015 *J. Vac. Sci. Technol.* A **33** 061202
[25] Chindaudom P and Vedam K 1994 *Appl. Opt.* **33** 2664
[26] Umeda M, Tezuka Y, Shin S and Yagishita A 1996 *Phys. Rev.* B **53** 1783
[27] Lyddane R, Sachs R and Teller E 1941 *Phys. Rev.* **59** 673
[28] Zinenko V and Zamkova N 2000 *Phys. Solid State* **42** 1348
[29] Zhong W, King-Smith R and Vanderbilt D 1994 *Phys. Rev. Lett.* **72** 3618
[30] Wang Y, Lee S, Zhang L, Shang S, Chen L Q, Derecskei-Kovacs A and Liu Z K 2014 *Chem. Phys. Lett.* **607** 81
[31] Mooradian A and Wright G 1966 *Phys. Rev. Lett.* **16** 999
[32] Liu Y, Wang Z, Wu M, Sun Q, Chao M and Jia Y 2015 *Comput. Mater. Sci.* **107** 157
[33] van Roekeghem A, Carrete J and Mingo N 2016 *Phys. Rev.* B **94** 020303
[34] Szigeti B 1959 *Proc. R. Soc.* A **252** 217
[35] Szigeti B 1963 *Solid State Commun.* **1** 184
[36] Lax M and Burstein E 1955 *Phys. Rev.* **97** 39
[37] Gao F *et al* 1991 *Phys. Rev.* B **43** 10383
[38] Ridou C, Rousseau M and Gervais F 1986 *J. Phys. C: Solid State Phys.* **19** 5757
[39] Lipson H G, Bendow B, Massa N E and Mitra S S 1976 *Phys. Rev.* B **13** 2614
[40] Jasperse J, Kahan A, Plendl J and Mitra S 1966 *Phys. Rev.* **146** 526
[41] Harrington J A and Hass M 1973 *Phys. Rev. Lett.* **31** 710
[42] Eldridge J 1972 *Phys. Rev.* B **6** 1510
[43] Hardy J R and Karo A 1982 *Phys. Rev.* B **26** 3327
[44] Zhu D, Robert A, Henighan T, Lemke H T, Chollet M, Glownia J M, Reis D A and Trigo M 2015 *Phys. Rev.* B **92** 054303
[45] Kozina M, van Driel T, Chollet M, Sato T, Glownia J, Wandel S, Radovic M, Staub U and Hoffmann M 2017 *Struct. Dyn.* **4** 054301
[46] Hong J, Kahng D, Shin J, Kim H and Khim Z 1998 *J. Vac. Sci. Technol.* B **16** 2942
[47] Paruch P, Tybell T and Triscone J M 2001 *Appl. Phys. Lett.* **79** 530
[48] Chu Y H, Cruz M P, Yang C H, Martin L W, Yang P L, Zhang J X, Lee K, Yu P, Chen L Q and Ramesh R 2007 *Adv. Mater.* **19** 2662
[49] Balke N, Choudhury S, Jesse S, Huijben M, Chu Y H, Baddorf A P, Chen L Q, Ramesh R and Kalinin S V 2009 *Nat. Nanotechnol.* **4** 868